Numerical Optimization of Single-Mode Photonic Crystal VCSELs

Péter Nyakas[1], Tomofumi Kise[2],
Tamás Kárpati[1], and Noriyuki Yokouchi[2]

(1) Furukawa Electric Institute of Technology, Hungary

(2) Furukawa Electric Corporation, Japan

(NUSOD '08, WB5)

Outline

Introduction

- Photonic crystal (PhC) VCSELs
- Single-mode condition defined by waveguiding
- Loss discrimination effect

3-D coupled simulation model

- Electro-thermal models
- Direct solution of Helmholtz equation
- Rate-equation approach

Results

- Current and temperature distributions
- Optical mode profiles and loss discrimination
- Static light power versus current (L-I) diagrams

Summary and outlook

Photonic Crystal VCSELs

- Optical confinement: PhC and optionally oxide aperture
- Electrical confinement: proton-implant or oxide aperture
- They potentially offer high-power single-mode operation.
- Design parameters: lattice constant (Λ, a), hole diameter (d) or diameter-to-pitch ratio, etching depth, and the diameter of the electrical aperture

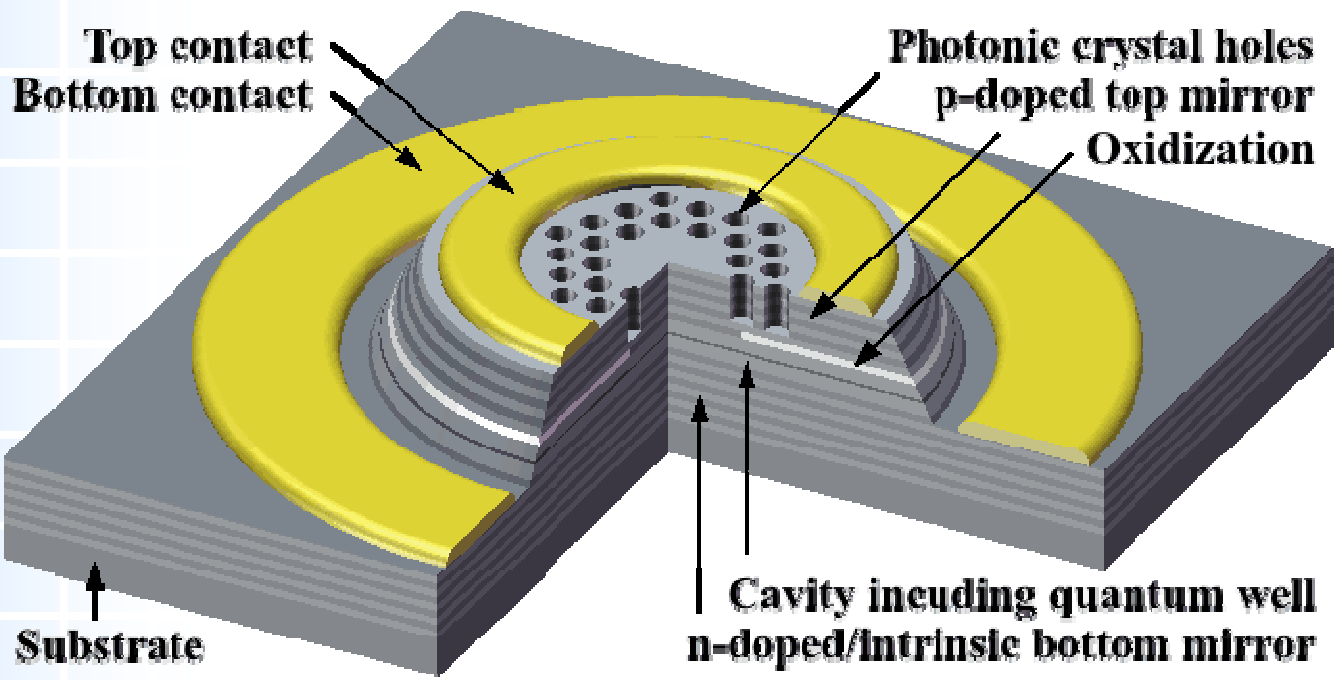

Single-Mode PhC-VCSELs

Normalized frequency parameter

$$V_{\text{eff}} = 2\pi r/\lambda \sqrt{n_{\text{eff}}^2 - (n_{\text{eff}} - \gamma\Delta n)^2} \qquad [1]$$

- n_{eff}: refractivity of core
- Δn: index change introduced by full PhC
- γ: etching depth factor (0–1)
- $V_{\text{eff}} < 2.405$ corresponds to the single-mode regime [2]

Normalized propagation constant

- 2-D Helmholtz equation for the transverse cross section (fully etched VCSEL)

$$B = \left(\beta_{\text{mode}}^2 - \beta_{\text{core}}^2\right) / \left(\beta_{\text{clad}}^2 - \beta_{\text{core}}^2\right) \qquad [3]$$

- β: propagation constant
- $B_{\text{LP}_{01}} < 0.57$ corresponds to the single-mode regime [3]

[1] N. Yokouchi *et al.*, IEEE JSTQE, **9**, p. 1439 (2003)
[2] A. J. Danner *et al.*, APL, **82**, p. 3608 (2003)
[3] P. S. Ivanov *et al.*, JOSAB, **20**, p. 2442 (2003)

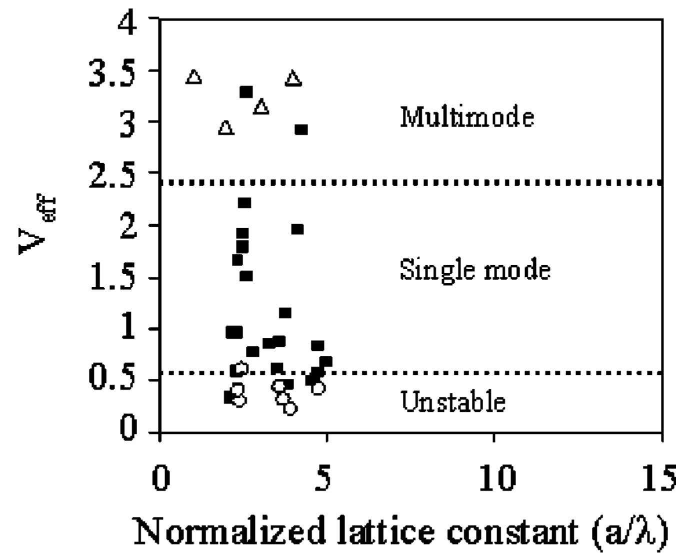

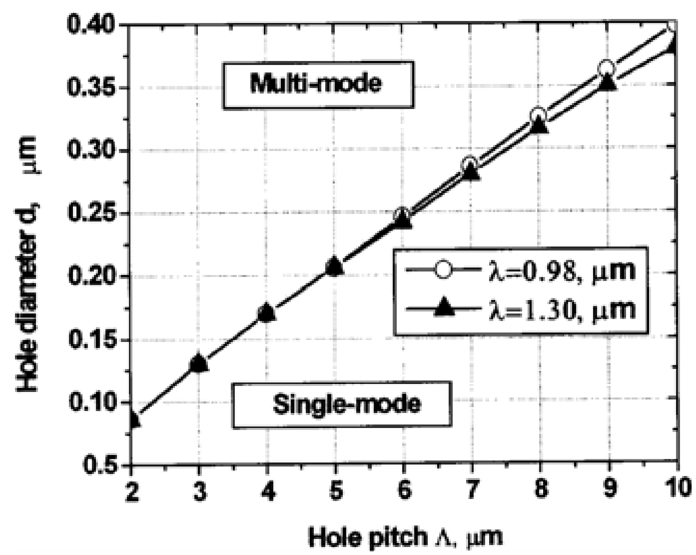

Modal Loss Effect

- It was shown experimentally [4] and with simulations that not only the modes' confinement but also their losses influence the single-mode condition.
- Plane wave admittance method [5] and finite element method [6] were applied, both for cold-cavity case.

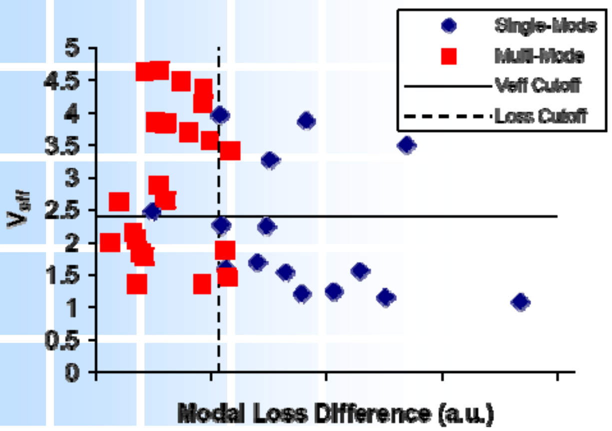

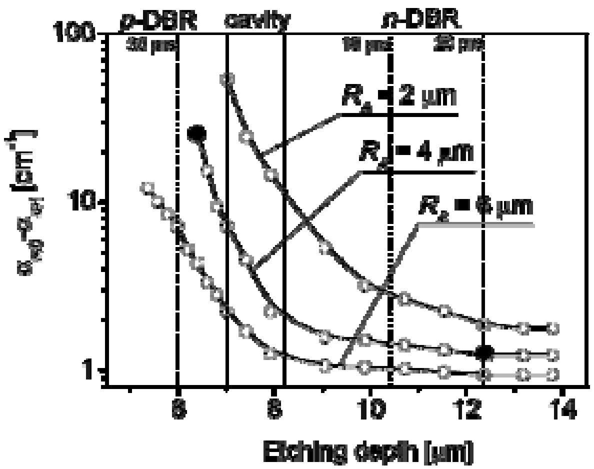

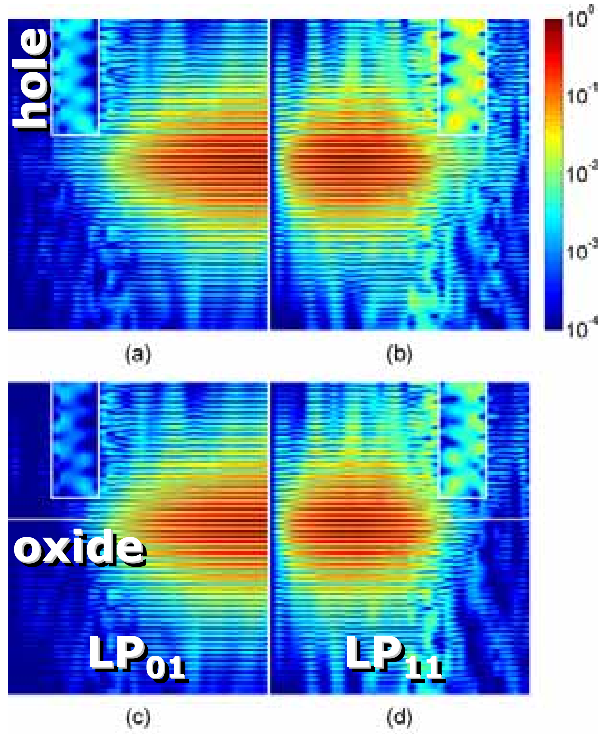

[4] D. F. Siriani *et al.*, LEOS 2007, WZ3

[5] T. Czyszanowski *et al.*, Opt. Express, **15**, p. 5604 (2007)

[6] P. Nyakas, JLT, **25**, p. 2427 (2007)

Introduction

- Photonic crystal (PhC) VCSELs
- Single-mode condition defined by waveguiding
- Loss discrimination effect

3-D coupled simulation model

- Electro-thermal models
- Direct solution of Helmholtz equation
- Rate-equation approach

Results

- Current and temperature distributions
- Optical mode profiles and loss discrimination
- Static light power versus current (L-I) diagrams

Summary and outlook

Electro-Thermal Models

Electro-thermal equations [7]

- Laplace equation for the electrostatic potential (Φ)
- anisotropic electric conductivity (**σ**) for heterojunctions
- stationary solution of the heat conductivity equation with different heat sources (*R*)

$$\nabla\left(\boldsymbol{\sigma}\nabla\Phi\right)=0 \qquad c\rho\frac{\partial T}{\partial t}=\nabla\left(\boldsymbol{\kappa}\nabla T\right)+R_{\mathrm{nr}}+R_{\mathrm{Joule}}+R_{\mathrm{abs}}$$

Discretization

- definition of lateral regions by projecting all interfaces to the top plane
- setting up prism elements that respect all interfaces
- integration by finite volume method (box method)

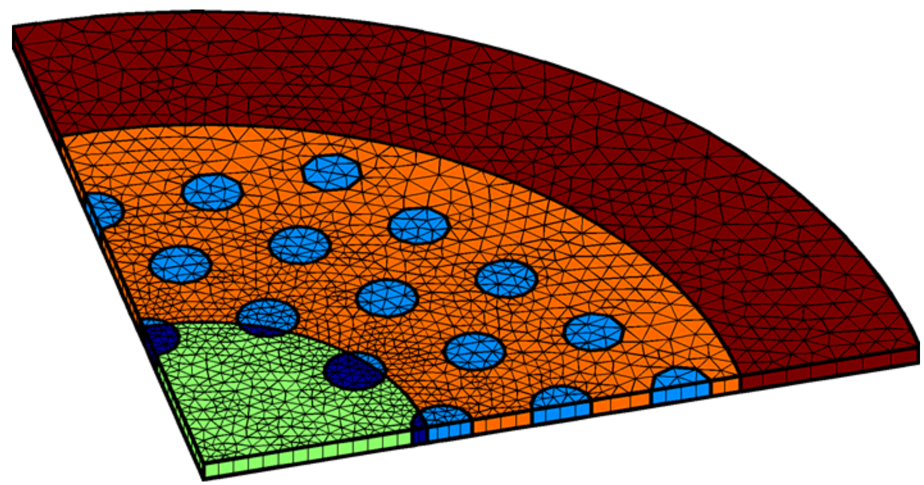

(green: aperture, orange: implant, deep red: contact and PML, blue: holes)

[7] P. Nyakas *et al.*, JOSAB, **23**, p. 1761 (2006)

Material Parameters

Temperature-dependent complex refractivity

- linear dependency of the real part of the index versus temperature
- its coefficient depends on the Al-composition of $Al_xGa_{1-x}As$, and $\frac{1}{n'}\frac{dn'}{dT}$ varies between $1.25–4\times10^{-4}$ 1/K [8]
- we used exponential temperature dependence for the imaginary part that corresponds to free-carrier absorption
- T_0 = 180 K was assumed irrespective of the composition due to the lack of more detailed experimental data [9]

Empirical gain function

$$g_i(n,T) = a_0 \ln\left(\frac{n}{n_0}\right)\left\{1-\left[\frac{\lambda_{gain}(T)-\lambda_i(T)}{\Delta\lambda}\right]^2\right\}$$

- the gain coefficient (a_0) and the transparency carrier density (n_0) can depend on temperature
- we assumed a parabolic effect of gain-to-cavity detuning

[8] M. Streiff *et al.*, IEEE JSTQE, **9**, p. 879 (2003)
[9] C. H. Henry *et al.*, IEEE JQE, **QE-19**, p. 947 (1983)

3-D Optical Mode Solver

Scalar and vectorial solutions

- finite volume method was used to solve the scalar Helmholtz equation [7],
- and finite element method was applied to solve the vectorial Helmholtz equation [6]

$$\Delta E = -\frac{\omega^2}{c_0^2}\varepsilon E$$

$$F(\mathbf{E}) = \frac{1}{2}\int_V \left[(\nabla \times \mathbf{E}) \mathbf{\Lambda}^{-1} (\nabla \times \mathbf{E}) - \frac{\omega^2}{c_0^2} \mathbf{E}\varepsilon\mathbf{E} \right] \mathrm{d}V$$

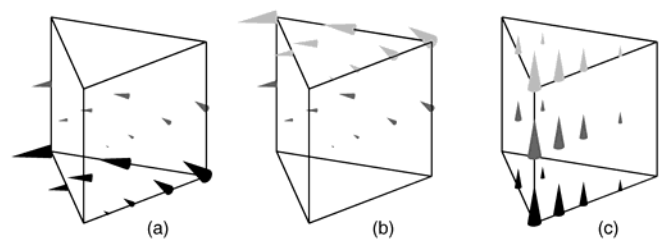

- the scalar solution is used here because of its lower memory and runtime demands

Symmetry boundary conditions

- a 30-degree section is enough to calculate the scalar fundamental and some higher modes of a hexagonal PhC lattice
- a quarter cross-section is needed for LP_{11} and other higher modes

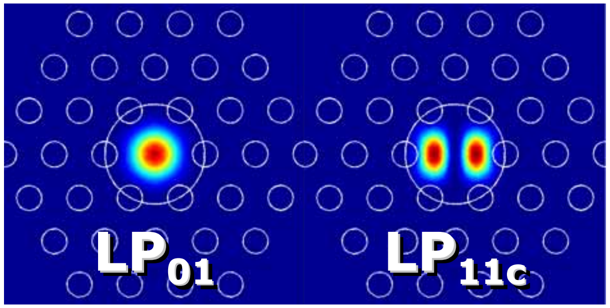

[6] P. Nyakas, JLT, **25**, p. 2427 (2007)

[7] P. Nyakas et al., JOSAB, **23**, p. 1761 (2006)

3-D Optical Mode Solver

Cold-cavity and active cavity descriptions

- optical gain is *not* included directly in the complex index when determining the laser resonator modes
- it is taken into account in the rate equation approach when following the evolution of the modes' power
- however, local free-carrier absorption loss in the mirrors is included in the refractive index
- the real part of the index is updated according to the local temperature when calculating the mode profiles

Algebraic problem

- the complex-symmetric generalized eigenproblem is solved with preconditioned shift-invert iteration
- the convergence speed and the memory allocation can be tuned with the drop tolerance [7]

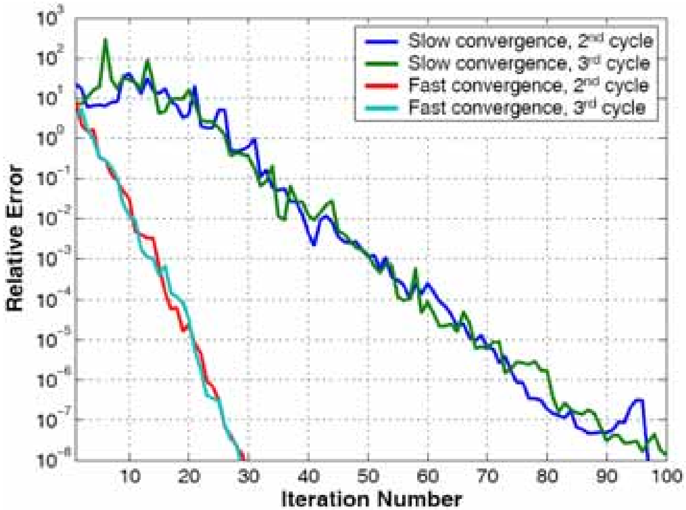

[7] P. Nyakas et al., JOSAB, **23**, p. 1761 (2006)

Multi-Mode Rate Equations

- cover local radiative and nonradiative recombinations, lateral carrier diffusion and spatial hole burning
- the stationary solution is found using an ODE-solver after spatial discretization

$$\frac{\partial n(\mathbf{r},t)}{\partial t} = \frac{\eta j(\mathbf{r},t)}{ed} - An - Bn^2 - Cn^3 + $$
$$+ D\Delta n - v_g \sum_i g_i(n)|E_i|^2 S_i$$

$$\frac{dS_i(t)}{dt} = \beta B \int_{QW} n^2 \mathrm{d}V + $$
$$+ v_g \left[\int_{QW} g_i(n)|E_i|^2 dV - L_i \right] S_i$$

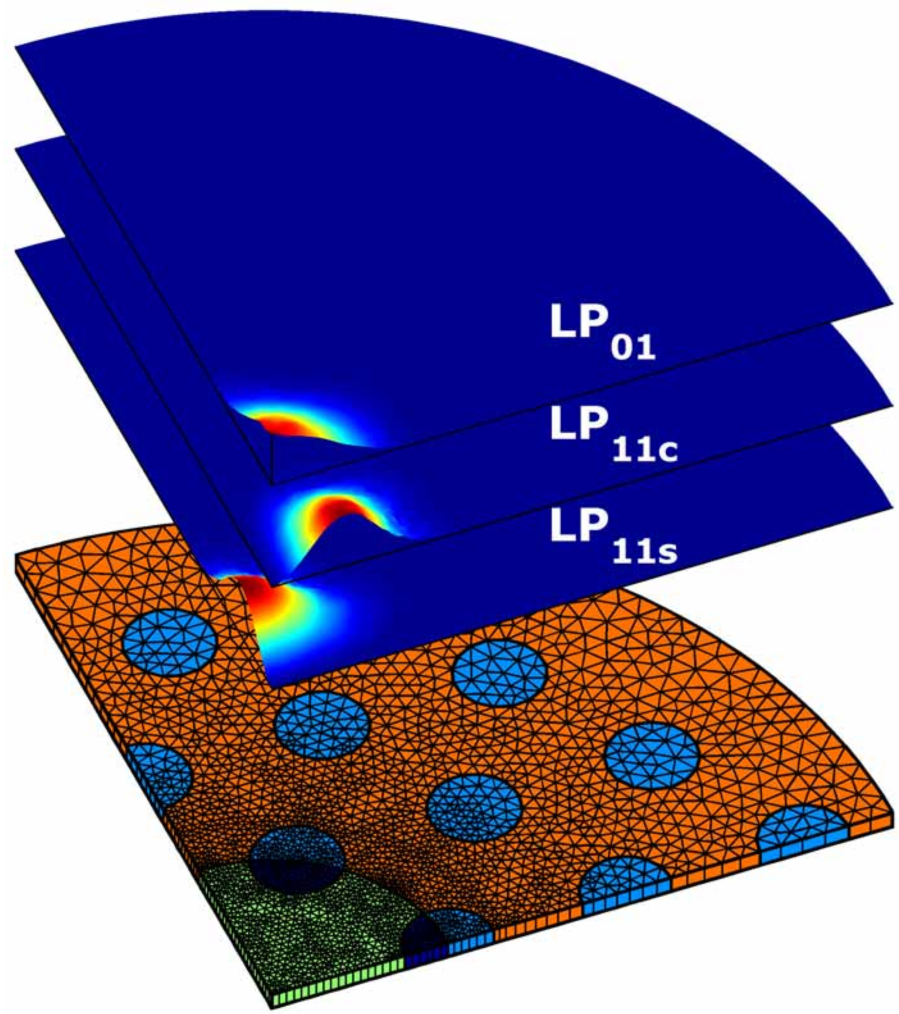

Coupled Simulations

Computer demands and simulation times

- it took about 2-3 GB memory and 20-60 minutes to find the fundamental mode once (30-degree section, 1.5m unknowns)
- it took about 10-25 GB memory and 10-30 hours to determine LP_{11} mode once (90-degree section, 4.2m unknowns)

Interpolation technique

- to accelerate the simulations for varying bias current,
- we estimated the temperature distribution at discrete points from the electro-thermal equations,
- and calculated the optical modes under these conditions
- the transverse mode profiles and the respective quantitative data were then interpolated for interior bias points

Introduction

- Photonic crystal (PhC) VCSELs
- Single-mode condition defined by waveguiding
- Loss discrimination effect

3-D coupled simulation model

- Electro-thermal models
- Direct solution of Helmholtz equation
- Rate-equation approach

Results

- Current and temperature distributions
- Optical mode profiles and loss discrimination
- Static light power versus current (L-I) diagrams

Summary and outlook

Target of Optimization

Fixed parameters

- design wavelength: 850 nm
- top-DBR: 30 pairs of p-doped $Al_{0.9}Ga_{0.1}As/Al_{0.2}Ga_{0.8}As$
- bottom-DBR: 35.5 pairs of n-doped $Al_{0.9}Ga_{0.1}As/Al_{0.2}Ga_{0.8}As$
- implant thickness: 12 pairs (about 1.5 μm)
- aperture diameter: 7.9 μm
- three rings of holes in a hexagonal pattern around a single defect
- hole diameter: 0.5 Λ
- we consider 2 modes

To be optimized

- lattice constant (3/4/5 μm) to obtain highest single-mode power in fundamental mode

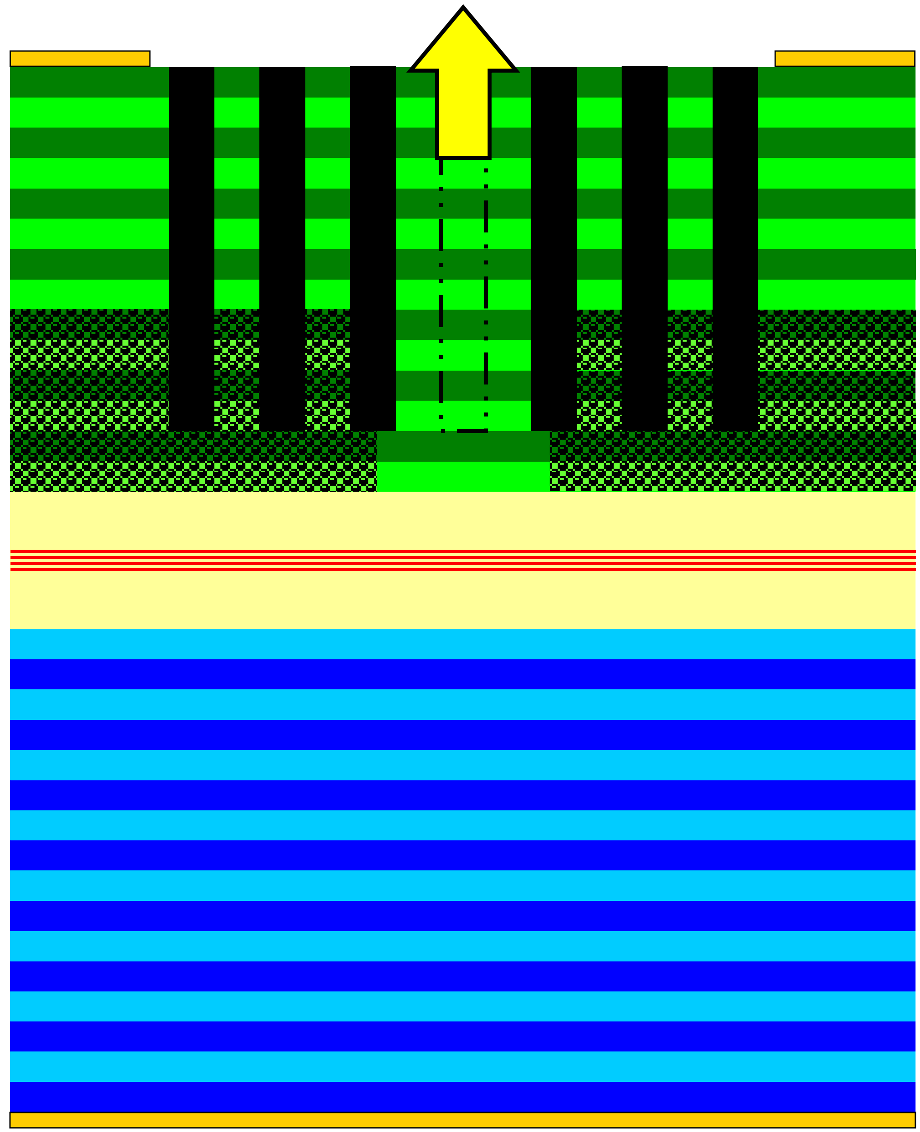

Temperature & Current Profiles

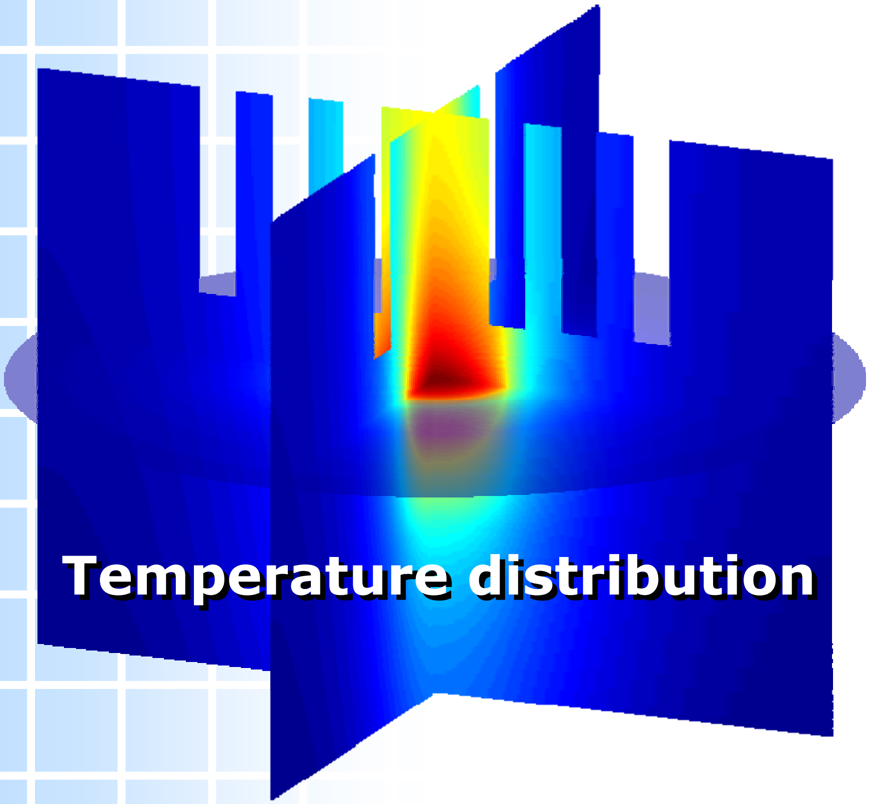

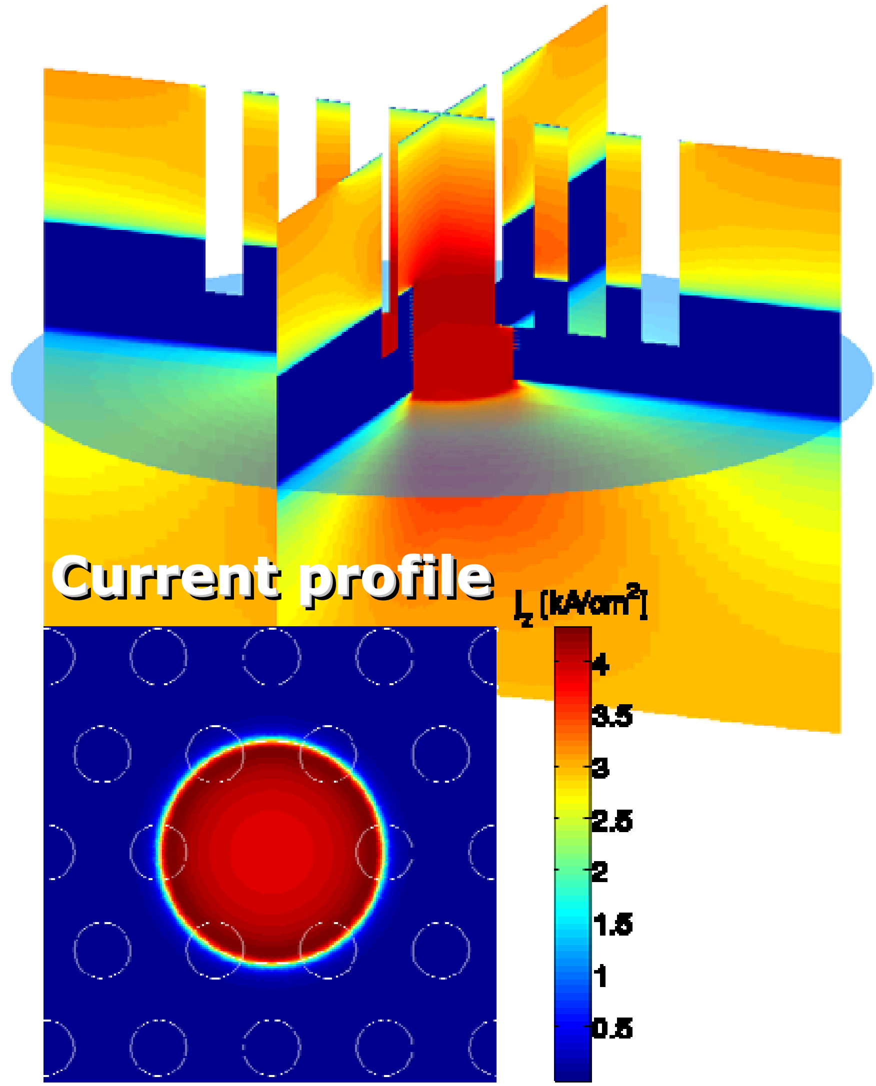

- The holes do not seem to impact drastically either the heat flow or the current flow.
- The electric conductivity may degrade also around the holes.

Thermal Lensing

Λ = 4 μm, 0/10/20 mW heat dissipation

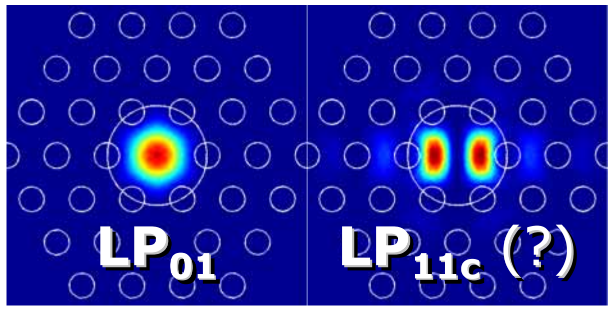

Λ = 3 μm,
10 mW heat
dissipation

Λ = 5 μm,
10 mW heat
dissipation

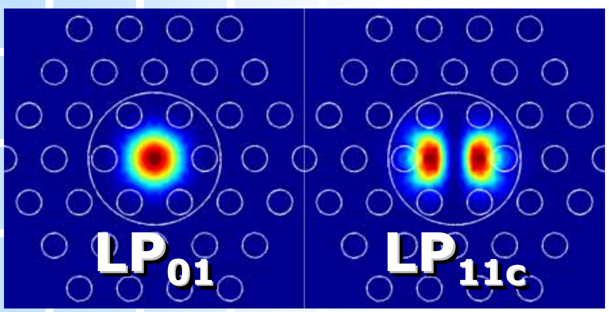

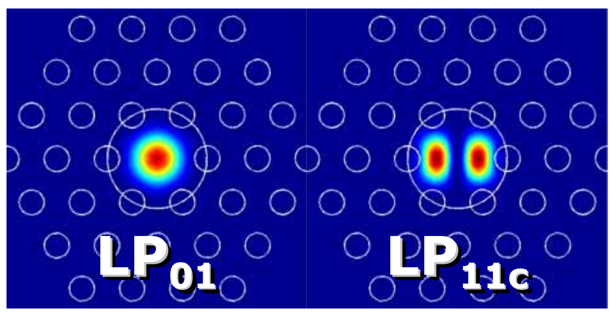

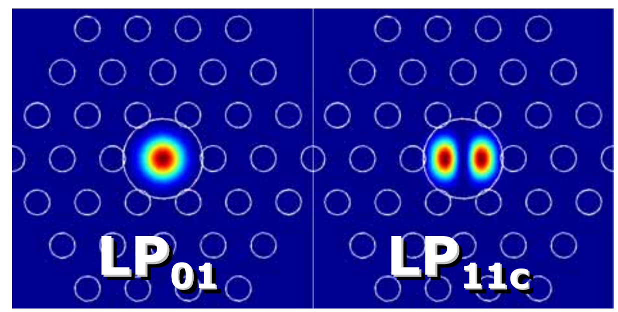

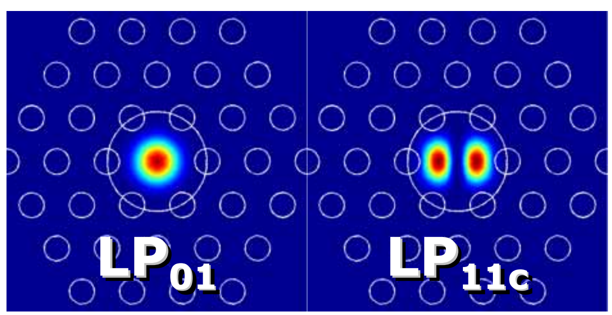

Optical Mode Properties

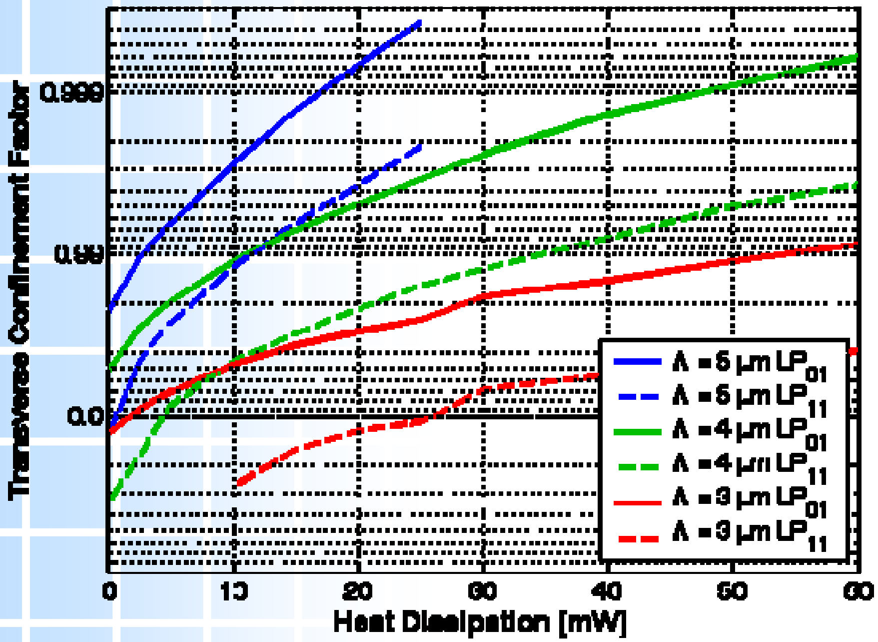

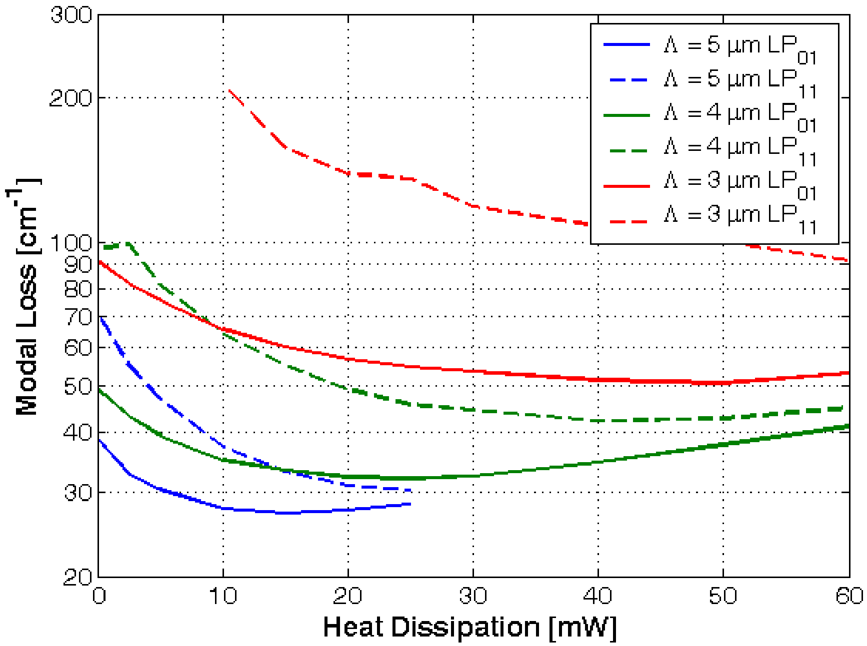

- the transverse confinement increases with larger lattice constant and increasing bias current
- modal discrimination increases as the lattice constant shrinks
- it depends on the structure which of the two effects is dominant

L-I Diagrams

Calculation

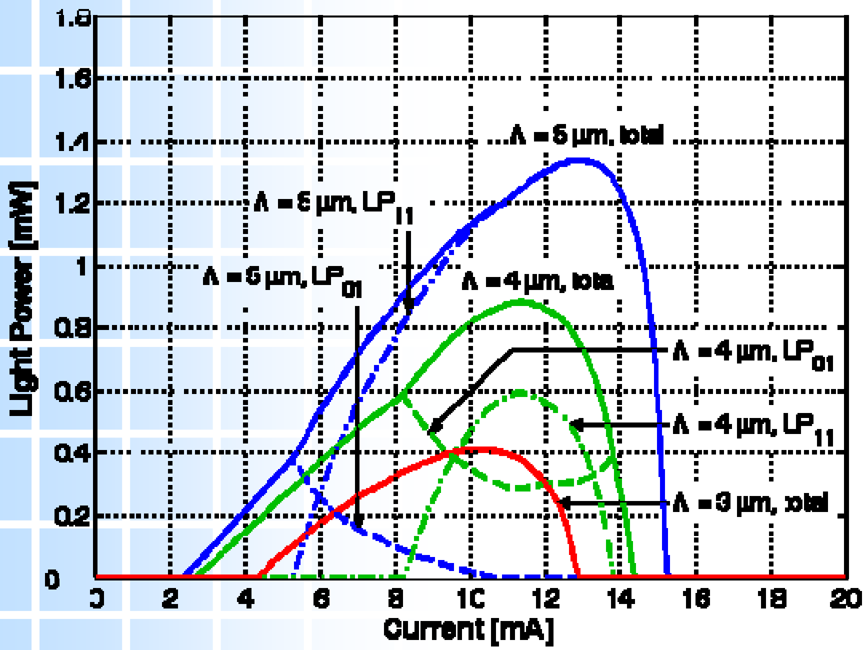

Measurement

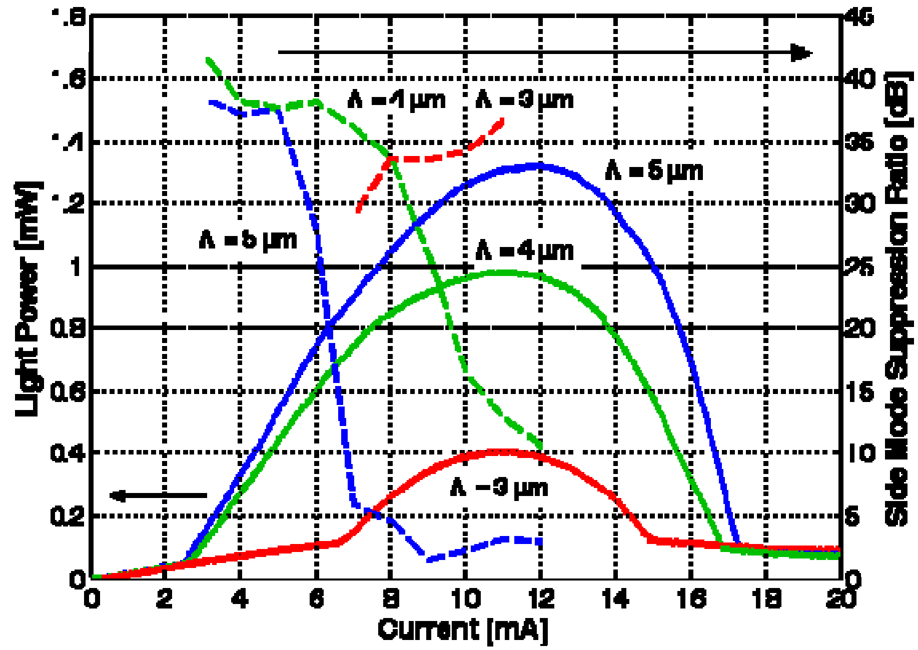

- the threshold current increases, and the slope decreases for smaller Λ due to higher optical loss and more wasted current
- single-mode operation can be maintained even if LP_{11} gets confined, but suffers from high optical loss
- simulation and experiment agree in the optimal Λ = 4 µm

Spatial Hole Burning

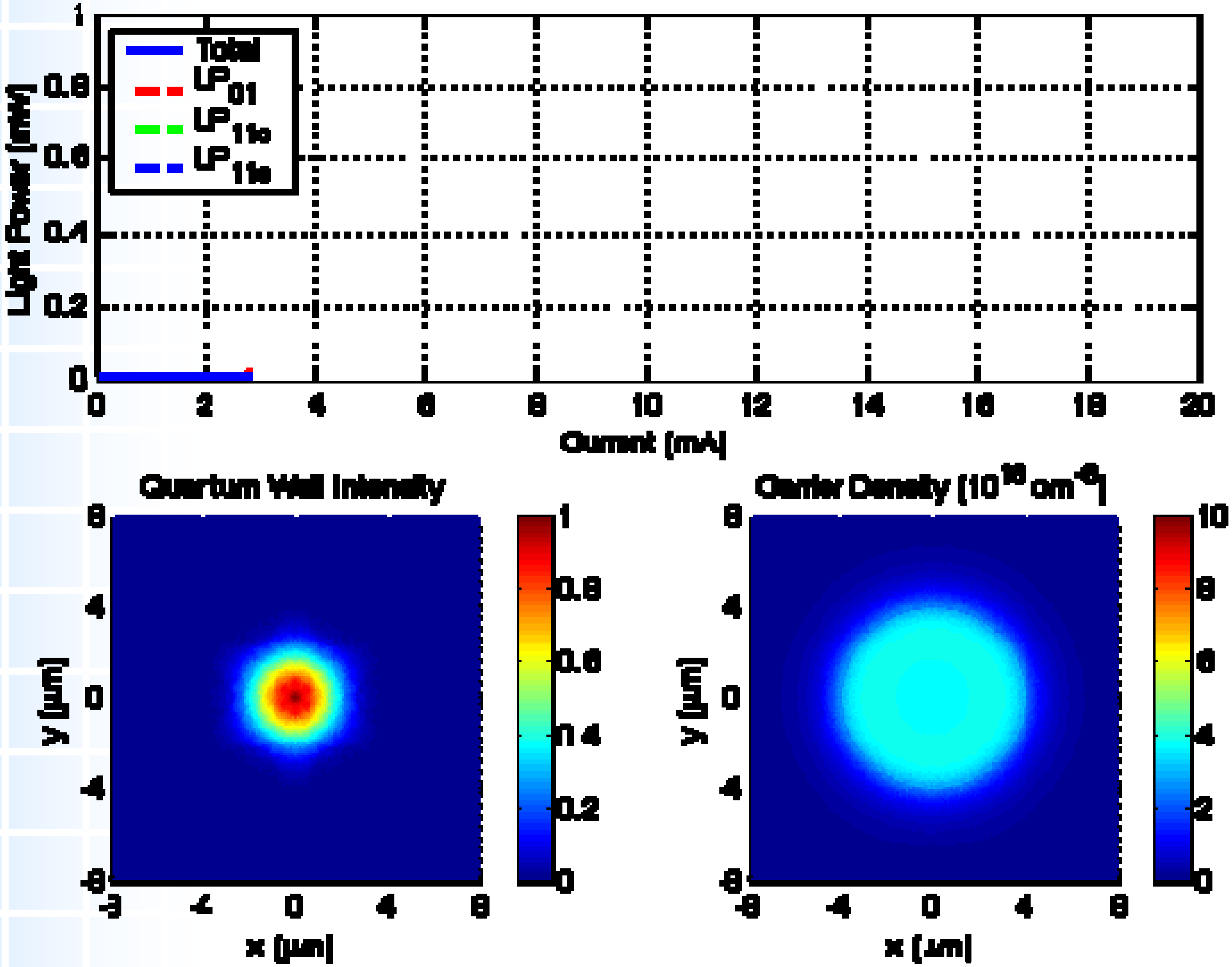

Summary and Outlook

Results

- 3-D coupled simulation model for PhC-VCSELs
- the confinement and the modal loss discrimination effects have been compared
- simulation and experiment have shown agreement in the optimal lattice constant that gives highest single-mode power

Further optimization

- optimal ratio of the diameter of the optical and electrical confinements
- an oxide aperture provides lower differential resistance,
- but it can influence the mode confinement and also the losses
- optimization of small-signal modulation response

Improve the electrical simulation

- drift-diffusion model aiming realistic semiconductor behavior
- check the dependence of the differential resistance on the holes' diameters, and determine the effective hole size